

Spin state of spin-crossover complexes: From single molecules to ultrathin filmsManuel Gruber,^{1,2,*} Vincent Davesne,^{1,2} Martin Bowen,¹ Samy Boukari,¹ Eric Beaurepaire,¹
Wulf Wulfhekel,^{2,3} and Toshio Miyamachi^{2,3,4}¹*Institut de Physique et Chimie des Matériaux de Strasbourg, Université de Strasbourg, CNRS UMR 7504, 23 rue du Loess,
BP 43, F-67034 Strasbourg Cedex 2, France*²*Physikalisches Institut, Karlsruhe Institute of Technology, Wolfgang-Gaede-Str. 1, 76131 Karlsruhe, Germany*³*DFG-Center for Functional Nanostructures, Karlsruhe Institute of Technology, 76131 Karlsruhe, Germany*⁴*Institute for Solid State Physics, University of Tokyo, 5-1-5 Kashiwanoha, Kashiwashi, Chiba 277-8581, Japan*

(Received 26 October 2013; revised manuscript received 5 February 2014; published 13 May 2014)

The growth of spin-crossover $\text{Fe}(1,10\text{-phenanthroline})_2(\text{NCS})_2$ molecules on $\text{Cu}(100)$ surfaces in the coverage range from 0.1 to 1.8 molecular layers was studied using a scanning tunneling microscope (STM) operated in ultrahigh vacuum at low temperature (≈ 4 K). STM imaging allowed us to extract the molecular adsorption geometry. While the first-layer molecules point their NCS groups toward the surface and their phenanthroline groups upwards, the adsorption geometry is reversed for the molecules in the second layer. For submonolayer coverages, a coexistence of molecules in the high- and low-spin states was found that is not correlated with the coverage. This coexistence is reduced for second-layer molecules, leading to a dominant spin state at low temperatures. Differential conductance spectra acquired at negative bias voltage on first- and second-layer molecules suggest that second-layer molecules are in the high-spin state and are partially electronically decoupled from the substrate. Furthermore, increasing the tip-to-sample voltage reduces the distance between the two lobes of the molecule. The current dependence of this effect suggests that a smooth spin crossover from a high- to a low-spin state occurs with increasing sample voltage. This analog spin-state switching is well described within a simple transition-state model involving modifications to the energy barriers between low- and high-spin states due to a tip-induced electric field through the Stark effect.

DOI: [10.1103/PhysRevB.89.195415](https://doi.org/10.1103/PhysRevB.89.195415)

PACS number(s): 68.37.Ef, 82.37.Gk, 75.30.Wx, 75.70.Rf

I. INTRODUCTION

The field of molecular electronics aims to utilize the properties of single molecules to build nanoscale electronic components [1]. For example, high-density-memory devices can be designed by exploiting the metastable states of a molecule [2]. In this case, one may consider the two spin states in spin-crossover (SCO) complexes. These complexes are composed of a central transition-metal ion surrounded by organic ligands whose spin state can be switched between a low-spin (LS) and a high-spin (HS) state by applying external stimuli such as temperature, light, pressure, magnetic or electric fields, or current [3–17]. To date, only a few studies report the successful sublimation of SCO complexes [15,16,18–24] due to the fragile nature of such complexes. These studies indicate that the intrinsic SCO property is usually preserved in thick films but depends on the electronic environment for ultrathin films and single molecules. This reflects a difference in the coupling strength between the molecules and the substrate, which itself arises in part from chemisorption [25,26]. Nevertheless, there are no thickness dependence studies of the molecule-substrate coupling from single molecules to ultrathin films.

In this work, we used $\text{Fe}(1,10\text{-phenanthroline})_2(\text{NCS})_2$ (Fe-phen) molecules composed of two phenanthroline groups and two thiocyanate groups as represented in Fig. 1(a). The molecule undergoes a thermal spin crossover from the LS state $S = 0$ to the HS state $S = 2$ [see Fig. 1(b)] that occurs in the bulk and in thin films [19] as temperature is increased

beyond 175 K. The transition is accompanied by changes in the iron-nitrogen bond lengths and angles [27,28] that lead to changes in molecular conformation [15].

In this paper, we use a scanning tunneling microscope (STM) to investigate the growth of Fe-phen on $\text{Cu}(100)$ and to provide insights into the origin of the coexistence of spin-state observed in the submonolayer regime [15]. We provide evidence of a partial electronic decoupling between Fe-phen and the copper substrate with increasing thicknesses. This decoupling appears to restore the SCO property of the molecules that is lost at the interface with Cu.

II. GROWTH AND ADSORPTION GEOMETRY OF $\text{Fe}(\text{PHEN})_2(\text{NCS})_2$

Clean and flat $\text{Cu}(100)$ surfaces were prepared by several cycles of Ar^+ sputtering (1.5 keV) and subsequent annealing to 450 °C. Fe-phen molecules were sublimated between 180 °C and 200 °C under ultrahigh vacuum conditions (deposition pressure of $p < 4.0 \times 10^{-10}$ mbar relative to a base pressure of $p < 2.4 \times 10^{-10}$ mbar), while maintaining the $\text{Cu}(100)$ substrate at a temperature of 45 °C.

Measurements were carried out in a home-built STM [29] in ultrahigh vacuum ($p < 2.0 \times 10^{-10}$ mbar) at low temperature ($T \approx 4$ K). STM tips were prepared by chemical etching of a tungsten wire and subsequent flashing in ultrahigh vacuum. Differential conductance dI/dV spectra were obtained with a lock-in technique using a modulation bias of 15 mV and a frequency of 723 Hz. When ramping the voltage, the feedback loop was opened.

Figure 2 represents STM images of Fe-phen on $\text{Cu}(100)$ with coverages ranging from 0.1 to 1.8 monolayers (ML).

*manuel.gruber@ipcms.unistra.fr

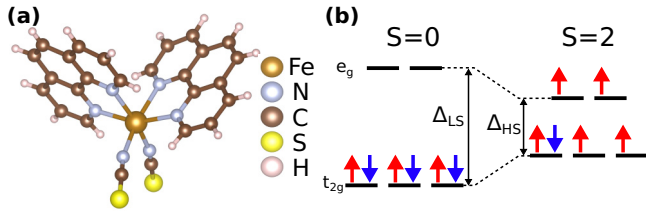


FIG. 1. (Color online) SCO Fe-phen molecule. (a) Model of the Fe-phen molecule consisting in a Fe ion surrounded by two phenanthroline groups and two thiocyanate groups. (b) Simplified electronic configuration of the Fe^{2+} ion $3d$ states where the octahedral ligand field lifts the degeneracy of the $3d$ orbitals and leads to t_{2g} and e_g orbitals. For a large ligand field, i.e., LS state, the energy difference between e_g and t_{2g} represented as Δ_{LS} is so large that the electrons occupy only the t_{2g} orbitals, leading to a total spin state $S = 0$. For a low ligand field, i.e., HS state, the energy splitting Δ_{HS} becomes smaller than the sum of the Coulomb and exchange energies, leading to an electronic arrangement such that $S = 2$.

As previously reported, single Fe-phen molecules appear as two lobes corresponding to the phenanthroline groups, and the spatial gap between the two lobes allows us to identify the spin state of a given molecule [15]. For example, in the inset to Fig. 2(a), the molecule with the larger interlobe gap is in the HS state while the other molecule is in the LS state. The surfaces shown in the large-scale topographies in Figs. 2(a)–2(d) reveal only very few impurities, indicating a clean and almost pure adsorption of Fe-phen onto Cu(100). Additionally, these figures indicate a layer-by-layer (Frank–van der Merwe) growth mode onto Cu(100).

At coverages of 0.1 and 0.4 ML [Figs. 2(a) and 2(b)], the molecules are rather isolated with very little clustering. This blocking of molecular diffusion may reflect a diffusion barrier on Cu that is higher than the room-temperature thermal energy [15]. However, as seen in Fig. 2(c), diffusion occurs for a coverage of 1.4 ML, leading to the formation of second-layer islands. We infer that the coupling of the second-ML molecules to the substrate is reduced, leading to a diffusion-barrier energy of the second-ML molecules that is low enough to allow their diffusion on top of the first layer. Since no significant molecular diffusion is observed at $T \approx 4$ K, any molecular diffusion must take place during and after deposition at room temperature, which leads to a molecular arrangement that is frozen upon subsequent cooling. When the coverage is

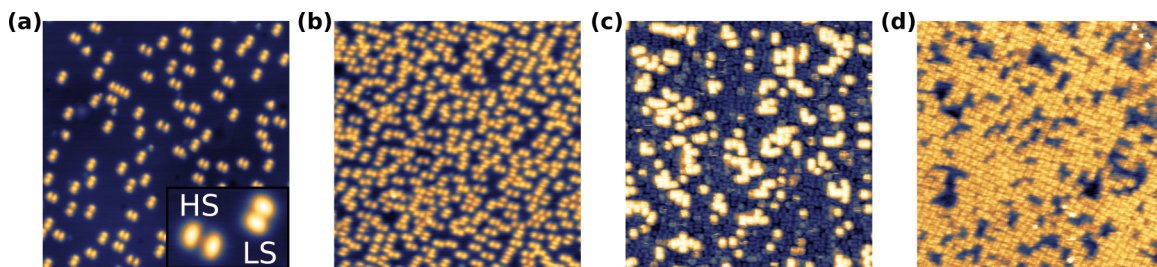


FIG. 2. (Color online) STM images of Fe-phen on Cu(100) at different coverages. The molecules remain isolated at low coverages of (a) 0.1 ML ($V = 0.1$ V, $I = 1.1$ nA) and (b) 0.4 ML ($V = 1.0$ V, $I = 15$ pA), while they form clusters at higher coverage of (c) 1.4 ML ($V = 1.0$ V, $I = 250$ pA). If the coverage is further increased, e.g., (d) 1.8 ML ($V = 1.8$ V, $I = 100$ pA), close to an integer number of ML, the molecules are organized as a short-range-ordered layer. The inset of panel (a) shows two single molecules with different spin states for clarity. Image sizes are 40×40 nm². The inset size is 6×4 nm².

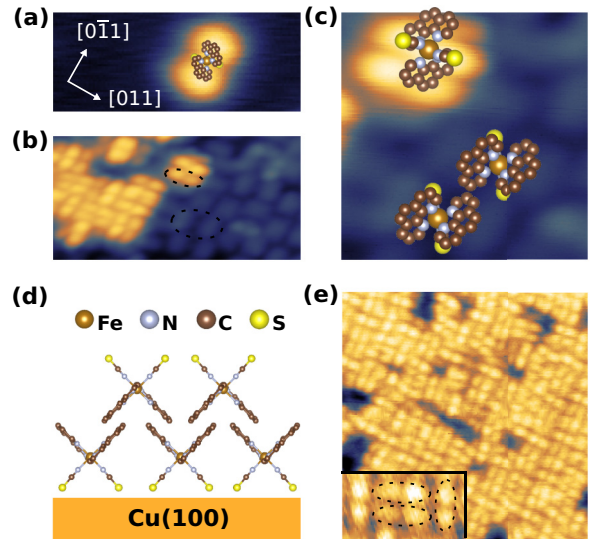


FIG. 3. (Color online) Coverage-dependent adsorption geometry of Fe-phen deposited onto a Cu(100) surface. (a) Model of Fe-phen superimposed on the topography of a single molecule. (b) Topography of 1.3-ML Fe-phen on Cu(100) where both the first and second ML are resolved. (c) Zoomed STM image of (b) with molecular models to indicate the different adsorption geometries between the first- and second-ML molecules. (d) Schematic of the proposed adsorption geometry of Fe-phen on Cu(100). (e) Topography of 1.8-ML Fe-phen on Cu(100) revealing a dense layer of molecules with short-range order. Inset: a zoomed topography (2.8×1.6 nm²) shows the common 3-molecule ordered pattern. The image sizes are (a) 6.6×2.7 nm² ($V = 0.2$ V, $I = 180$ pA), (b) 9.0×4.5 nm² ($V = 0.6$ V, $I = 200$ pA), (c) 3.1×3.1 nm², (d) 12×12 nm² ($V = 0.7$ V, $I = 70$ pA). The models of the molecules were created with VESTA [30].

increased up to 1.8 ML, islands grow further and coalesce to form a short-range-ordered molecular film as shown in Fig. 2(d).

In order to describe and understand the short-range structural order of this 1.8-ML film, we first recall how the molecules lie onto the Cu(100) surface. Figure 3(a) shows a single molecule in the LS state. A single Fe-phen molecular model [27] is scaled and superimposed onto the topography. Due to the broad π orbitals of the phenanthroline groups pointing upward [15], the apparent size of the molecule is significantly larger than that inferred from the model. Indeed,

STM at the low currents used here only probes the outermost part of the molecular wave function. Upon increasing the molecular coverage such that the maximum molecular density of the first-ML is achieved, as represented in Figs. 3(b) and 3(c) with a coverage of 1.4 ML, the effective size of the first-ML molecules still remains larger than that of the model molecule. On the other hand, the second-ML molecules look slightly smaller than the first-ML molecules, and also exhibit a different shape, which suggests a different adsorption geometry. We propose that the second-ML molecules lie upside down, with phen groups pointing downward, compared to first-ML molecules. This stacking, schematized in Fig. 3(d), enables π - π interactions between the phenanthroline groups of the first- and second-ML molecules as observed for the bulk [31] or inferred from STM experiments on other SCO complexes [16,22].

Increasing the coverage leads to dense areas with short-range order as emphasized in Fig. 3(e). In the small regions where the molecules are ordered, a molecular pattern can be deduced as represented by three encircled molecules in the inset to Fig. 3(e). This pattern reflects the fourfold symmetry of the substrate, and most probably favors intermolecular π - π interactions of the phenanthroline groups.

III. SPIN-STATE COEXISTENCE

A. Investigation of the spin-state coexistence

In our previous work [15], we demonstrated that the HS and LS states of Fe-phen deposited onto Cu(100) coexist at low temperatures. The coexistence of spin states has also been reported by Gopakumar *et al.* [16] for $[\text{Fe}(\text{bpz})_2(\text{phen})]$ on Au(111), Pronschinske *et al.* [22] for bilayer films of $\text{Fe}[\text{H}_2\text{Bpz}_2]_2\text{bpy}$ on Au(111), and Warner *et al.* [24] for $\text{Fe}[\text{H}_2\text{B}(\text{pz})_2]_2(\text{bipy})$ on Au(111). However, Bernien *et al.* [23] observed a thermal spin transition of a submonolayer of $[\text{Fe}^{\text{II}}(\text{NCS})_2\text{L}]$ (L: 1-6-[1,1-di(pyridin-2-yl)ethyl]-pyridin-2-yl-N,N-dimethylmethanamine) on a highly oriented pyrolytic graphite substrate without any indication of spin-state coexistence at low temperature. Thus, the spin-state coexistence of spin-crossover complexes depends on the electronic coupling between the SCO molecule and the substrate. As such, one must consider the specific case of every molecule/substrate pair, or system. In addition, the size of a SCO molecule in the HS state differs from the same molecule in the LS state, and leads to SCO cooperativity in bulk system. For single SCO molecules or for ultrathin film, the question arises as to whether the intermolecular elastic interactions can influence or even quench the spin-state coexistence.

In the constant-current topography of 0.1-ML Fe-phen on Cu(100) [see Fig. 4(a)], two different molecules with two different interlobe distances can be observed [see height profiles in Fig. 4(b)]. The molecules with the larger (smaller) interlobe distance have been previously ascribed as being in the HS (LS) state [15]. Referring to Fig. 4(c), the coexistence subsists at 0.5-ML coverage. However, this coexistence seems lost for molecules that form the second ML on Cu(100) as seen in Fig. 4(d). Indeed, if molecules with the same orientation are compared, there seems to be no difference in the interlobe gap. In Fig. 4(d), we indicate individual molecules with black

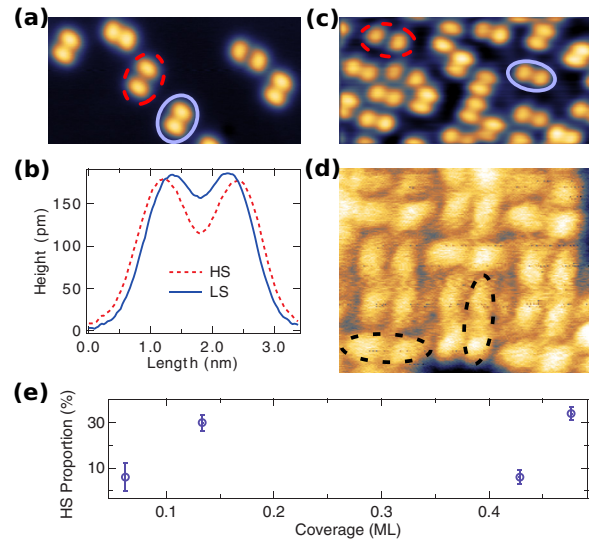


FIG. 4. (Color online) Study of the spin-state coexistence as a function of the coverage. (a) Constant-current topographies for coverage of 0.1-ML Fe-phen on Cu(100) ($V = 0.80$ V, $I = 500$ pA) where examples of HS and LS molecules are, respectively, indicated by dashed red and solid blue ellipses and (b) the line profiles along the long axis of the encircled molecules. Constant-current topography for coverage of (c) 0.5-ML Fe-phen ($V = 0.80$ V, $I = 500$ pA) and (d) 1.8-ML Fe-phen ($V = 0.30$ V, $I = 140$ pA) with example of second-ML molecules indicated by dashed black ellipses. (e) Proportion of HS molecules as a function of Fe-phen coverage. Each point corresponds to a different sample, and we used between 500 and 4000 molecules on each sample to determine the HS proportion. The coexistence of the spin states remains at submonolayer coverages but, in this regime, no direct correlation is found between the HS proportion and the coverage.

ellipses for clarity. We infer that a coexistence of spin states is sustained in the first-ML molecules while the second-ML molecules appear to be fixed into a dominant spin state. The first layer would act as a decoupling layer from the substrate [16], in analogy to CuN on Cu(100) [15] so as to increase intermolecular effects within the second layer such as cooperativity. Since the second-ML molecules are upside down, we are reluctant to deduce the spin state merely from the topography (see next section).

While the origin of the observed coexistence remains unknown for submonolayer coverages, the coupling between the molecules and the copper substrate, and more precisely the S-Cu bonding, is crucial as it prevents the molecules from relaxing into their ground (i.e., LS) state at $T \approx 4$ K. In Fig. 4(e), the proportion of Fe-phen molecules in the HS state on Cu(100) is plotted as a function of molecular coverage. The plot contains only a few data points, but it is rather clear that there is no direct correlation between the HS proportion and the molecular coverage. Furthermore, the HS proportion adopts the two discrete values of 5% or 30%. This suggests that the spin-state coexistence originates from the properties of the system rather than from a low-temperature frozen spin state, in agreement with the study reported by Pronschinske *et al.* [22].

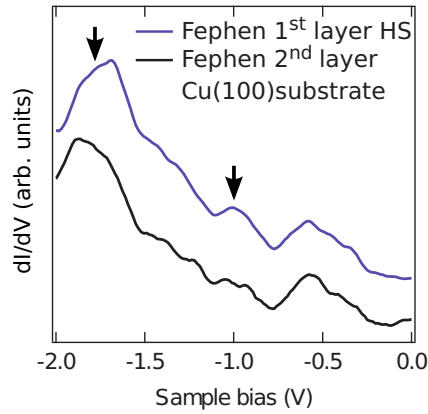


FIG. 5. (Color online) Differential conductance dI/dV spectra taken on a sample with 1.4 ML of Fe-phen on Cu(100), on top of a first-ML HS Fe-phen molecule and on top of a second-ML molecule. Peaks in the calculated Fe-ion density of states of first-ML molecules [25] are indicated by arrows for comparison. The spectrum of the second layer is multiplied by a factor 4 for clarity. The spectra are smoothed to remove nonphysical variations.

B. Identification of the spin state

The HS or LS character of a given molecule of the first ML can be identified using scanning tunneling spectroscopy (STS) as well as topography [15]. In the case of STS, the differential conductance of the HS molecules exhibits a Kondo resonance near the Fermi level that is absent for the LS molecules. As mentioned above, the molecules of the second ML exhibit a homogeneous spin state that cannot be simply deduced by topography since the molecule is now upside down. However, we note that, on one hand, the study of the HS proportion as a function of the Fe-phen coverage shown in Fig. 4(e) reveals a HS proportion between 5% and 30% for molecules composing the first ML. On the other hand, the x-ray absorption spectroscopy (XAS) study of approximately 2-ML Fe-phen on Cu(100) discussed in Ref. [15] indicates a much higher HS proportion of 46%. If we assume that the spin state of the first-ML molecules is not changed upon adsorption of second-ML molecules, simple algebra calculations suggest that the second-ML molecules are dominantly in the HS state. In order to reinforce the identification of the dominant spin state of the second ML, and since HS and LS molecules differ in their density of states, we carried out STS on 1.4 ML of Fe-phen on Cu(100) and compared it to its first-ML counterpart.

As a reference, STS carried out on the center of a first-ML HS molecule (see Fig. 5) exhibits peaks at -1.8 , -1.0 , and -0.6 eV, which is in good agreement with the calculated Fe-ion density of states of HS Fe-phen/Cu(100) [25]. Note that no peaks can be recognized in the unoccupied part (positive sample-bias voltage; data not shown) due to the strong tunneling background. There is no correspondence with the theory for the peak at -0.6 eV, which could originate from the Cu(100) substrate.

STS acquired atop a second-ML molecule's center is similar to the spectrum of a HS molecule in direct contact to the substrate. Thus, the second-layer molecules can be ascribed as being in the HS state in agreement with XAS results in

Ref. [15]. However, the peak at -1.8 eV of the first-ML molecule is slightly shifted to lower energies for the second-ML molecules. This shift, which suggests a lower-energy state for second-ML molecules compared to first-ML molecules, most probably reflects the reduced influence of the substrate on the second layer compared to the first layer.

C. Origin of the spin-state coexistence

The presented results indicate that the first-ML molecules directly anchored to the substrate exhibit a spin-state coexistence. On the other hand, second-ML molecules seem to be in a dominant spin state. XAS and STS results identify the second-ML molecules as being mostly in the HS state, in contrast to Fe-phen molecules which in bulk form are in the LS state at $T \approx 4$ K. The HS state might be induced by the geometry of the system through the position and orientation of the phenanthroline groups. Moreover, Félix *et al.* [32] developed a thermodynamic model for nanoparticles including the surface energy of HS and LS. They show that, for small enough nanoparticles, the model leads to a nonthermally switchable residual HS fraction in a proportion that depends on the difference between the HS and LS surface energies. The residual HS proportion can reach values up to 100% and would be in agreement with the dominant HS state of the second ML that we observe at low temperature.

As SCO is related to geometric modifications, the origin of the spin-state coexistence of the first layer could come from the adsorption geometry, and more precisely from the adsorption site and the strong bonding of sulfur on Cu. Topographies of Fe-phen molecules in HS and in LS states on atomically resolved Cu(100) surface are shown in Figs. 6(a) and 6(b), respectively. From the topographies, it is not possible to determine the adsorption sites of the sulfur ions as they are hidden by the phenanthroline groups. However, the distance between the two sulfur ions is known to decrease when going from a HS state to a LS state [27]. In addition, the center of the HS molecule, i.e., the position of the Fe ion, is positioned on top of a hollow site while the center of the LS molecule is on top of a bridge site, which suggests different adsorption sites for both spin states. Thus, once the molecule is adsorbed on copper, the spin state is fixed by the adsorption site, and switching the spin state of the molecules would require an energy sufficient to change the adsorption site. We present in Figs. 6(c) and 6(d) typical data sets corresponding to unsuccessful switching attempts on HS and LS molecules, respectively. The experiment consists in repeatedly scanning the same line along the long axis of the molecule while incrementally increasing the sample voltage from 0.1 to 2.0 V. This experiment has been reproduced for different tunneling currents (not shown) but no drastic change caused by the sample voltage can be monitored. Hence, no spin-state switching is achieved, as mentioned in Ref. [15]. The absence of switching could be explained by an insufficient energy transferred to the system in order to alter the molecule's adsorption site. Applying even larger sample voltage results in the destruction of the molecule as the iron-nitrogen bonds of Fe-phen might not withstand the energy applied to the system.

If the adsorption site of the molecule is modified, e.g., through a tip-induced lateral manipulation of the molecule, the

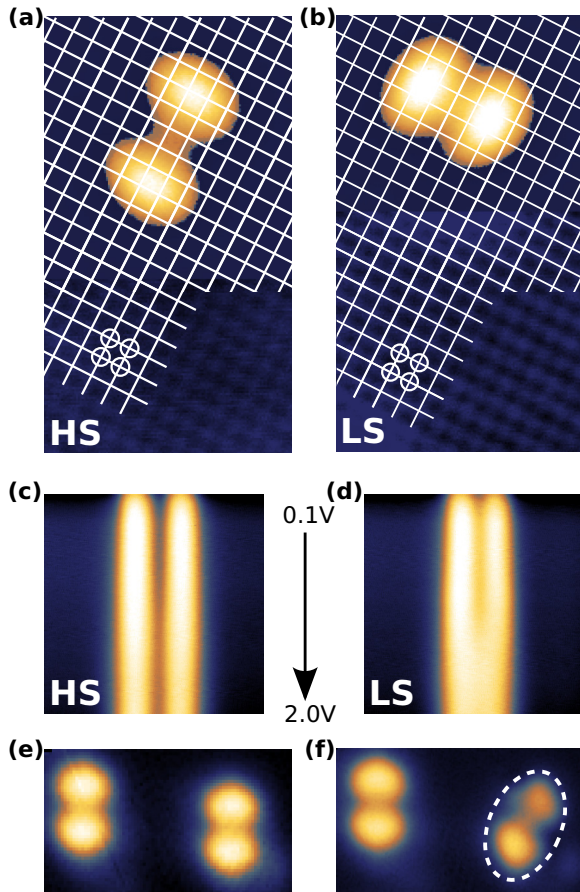


FIG. 6. (Color online) Spin-state switching attempts of first-ML Fe-phen on Cu(100). Topographies of single (a) HS Fe-phen and (b) LS Fe-phen molecules atop an atomically resolved Cu(100) surface so as to reveal the molecule's adsorption sites. The iron ion of the HS (LS) molecule is sitting on top of a hollow (bridge) position. Intersections of lines represent the center of a Cu atom. Four Cu atoms are encircled in each topography for clarity. Sample voltage dependencies of the STM height profile for the (c) HS and (d) LS states. (e) Topography before and (f) after a switching attempt from a LS to HS state by lateral tip manipulation. The manipulated molecule is encircled in an ellipse. Image sizes are (a) and (b) $4.8 \times 5.0 \text{ nm}^2$, (c) and (d) 6.0 nm , (e) and (f) $4.8 \times 2.8 \text{ nm}^2$.

switching from a LS state [molecule on the right in Fig. 6(e)] to a HS state [molecule on the right in Fig. 6(f)] is possible. However, the final orientation of the molecule was tilted by 45° compared to usual orientations of the molecules [see Fig. 2(a)], so that the conclusion of a final HS state after tip manipulation is not straightforward.

IV. SPIN CROSSOVER

A. Results

The coupling between the molecule and the substrate seems to be the dominant parameter in successfully performing spin-state switching. The spectroscopic results in Fig. 5 also suggest that the first layer reduces the influence of the substrate on the second-layer molecules. This is in analogy to the experiment with the same molecule on CuN/Cu(100) [15],

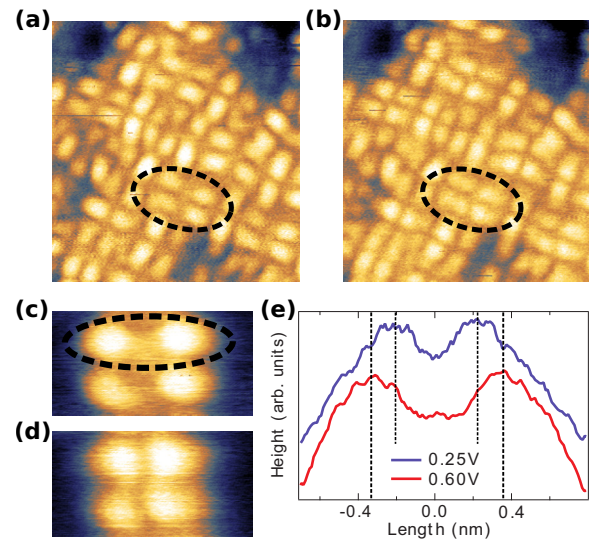


FIG. 7. (Color online) Topography acquired atop Fe-phen (1.8 ML) on Cu(001) at (a) low voltage (0.40 V) or at (b) higher voltage (0.70 V). A pair of molecules is indicated by an ellipse for clarity. The interlobe distance of a single molecule decreases with increasing voltage. Zoom on a pair of molecules at (c) low voltage (0.25 V) and at (d) higher voltage (0.60 V). A single molecule is indicated for clarity. (e) Height profiles of the upper molecule in topographies (c) and (d). The STM height profile at 0.25 V is shifted for clarity. Image sizes are (a) $5.50 \times 5.80 \text{ nm}^2$ ($V = 0.40 \text{ V}$, $I = 1.74 \text{ nA}$), (b) $5.50 \times 5.80 \text{ nm}^2$ ($V = 0.70 \text{ V}$, $I = 1.74 \text{ nA}$), (c) $2.40 \times 1.25 \text{ nm}^2$ ($V = 0.25 \text{ V}$, $I = 130 \text{ pA}$), (d) $2.40 \times 1.25 \text{ nm}^2$ ($V = 0.60 \text{ V}$, $I = 130 \text{ pA}$).

a molecule/substrate pair for which electrical switching is possible. The required energy to switch the spin state of the second-ML molecules would be of the order of the π - π interactions between the phenanthroline groups of the first and second ML, which is much lower than those mediated by the sulfur-copper bond. Hence, despite the negative results on first-ML molecules, it might nevertheless be possible to switch the spin state of the second-ML molecules through external stimuli. Gopakumar *et al.* [16] have also reported a spin crossover of a second-ML Fe(bpz)₂(phen) when decoupled from the Au(111) substrate by the first monolayer of molecules.

Regarding the second ML of Fe-phen on Cu(100), the spectroscopy and the reduced spin-state coexistence suggest a partial decoupling of the molecules from the substrate, so that a spin transition can be expected. We present topographies of the same area observed at 0.4 and 0.7 V in Figs. 7(a) and 7(b), respectively. The distance between the two lobes of a single molecule decreases when increasing the sample voltage, opposed to the same experiment on first-ML Fe-phen. Upon thereafter decreasing the applied voltage, the interlobe gap increases again and returns to its initial state (data not shown). Zoomed topographies on a pair of molecules subject to low- and higher-bias voltage are shown in Figs. 7(c) and 7(d), and the corresponding extracted height profiles are shown in Fig. 7(e). The molecular shape is clearly changed. However, no topographical change is observed at negative voltage (data not shown).

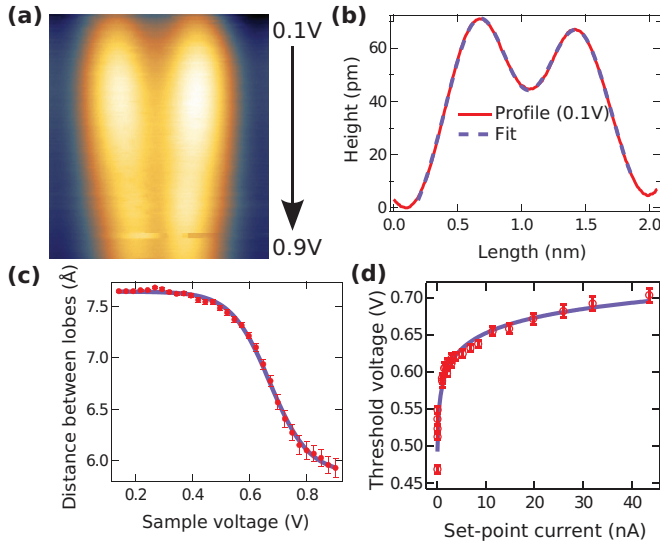


FIG. 8. (Color online) (a) Sample voltage dependencies of the STM height profile for a second-ML Fe-phen molecule on Cu(100). The image width is 2.06 nm ($I = 25.9$ nA). (b) Extracted STM height profile at 0.1 V from the data of panel (a). The solid red line corresponds to the profile and the dashed blue line represents the fit using Eq. (1). (c) Interlobe distance extracted from the fit of (b) as a function of the sample voltage (red data points) together with a fit (solid blue) using $d(V) = \text{base} + \frac{\text{max}}{1 + \exp(\frac{V_{Th} - V}{\text{rate}})}$ (fitting parameters: base = 7.641 ± 0.008 , max = -1.763 ± 0.025 , $V_{Th} = 0.670 \pm 0.003$, and rate = 0.068 ± 0.002). (d) Threshold voltage as a function of the tunneling current (red data points) on numerous data sets like that of panel (a) fitted with Eq. (10) (solid blue line).

The voltage-induced modification of the interlobe distance could originate from abrupt changes in the (orbital) density of states or from the expected spin crossover from a HS state at low voltages to a LS state at higher voltages. In the latter case, the question of the absence of the metastable LS state at low voltages arises, which can be answered by a lower potential barrier between the two spin states. Indeed, if we consider that the spin state coexistence of first-ML molecules, i.e., the existence of a potential barrier between the two states, originates from the adsorption site, i.e., the S-Cu bonding, it is reasonable to think that, in the case of a phen-phen bonding, this barrier becomes much lower.

Further experiments were carried out in order to more precisely detect the voltage at which the topographic changes occur. To do so, the height profile along the long axis of the molecule was continuously scanned while increasing the sample voltage, which lead to images such as in Fig. 8(a) [see also Figs. 6(c) and 6(d)]. From the acquired image, averaged height profiles are extracted for a given voltage [see an example in Fig. 8(b)] and fitted with a double Gaussian function:

$$Ae^{-\frac{(x-x_1)^2}{\sigma_1^2}} + Be^{-\frac{(x-x_2)^2}{\sigma_2^2}} + \text{const}, \quad (1)$$

in order to extract the positions x_1 and x_2 of the two lobes. As seen in Fig. 8(b) for the example of 0.1 V, Eq. (1) nicely fits the height profile. We present in Fig. 8(c) the bias voltage dependence of the interlobe distance $d(V) = x_2(V) - x_1(V)$. At low voltages, the distance between the lobes is maximal,

about 7.6 Å, and is more or less stable until 0.5 V. At higher voltages, $d(V)$ decreases smoothly and ends with a plateau at ≈ 6.0 Å. The interlobe gap at the two plateaus can slightly vary with different tips, but the shrinking of the lobes is always about 25%. We observe no variation of the interlobe distance at negative sample voltage (data not shown). The distance between the lobes as a function of the sample voltage is then fitted using a sigmoid function in order to extract the threshold voltage V_{Th} at which half of the shrinking occurs.

A set of STM height profiles versus sample-voltage images [e.g., Fig. 8(a)] were recorded for different set-point currents. The extraction of the height profiles and the fitting procedures were then reproduced for each of the acquired images. In the resulting tunneling current dependence of V_{Th} plotted in Fig. 8(d), we see that the higher the tunneling current, the higher the threshold voltage needed.

B. Possible origins of the bias-induced change in interlobe distance of the second-ML Fe-phen

In this section, we discuss our observation of bias-induced changes in interlobe distance in terms of two possible origins: (a) a change in the orbital that is probed; and (b) a dynamic averaging of the interlobe distance corresponding to the two HS and LS molecular states. Throughout this discussion, we emphasize that the spin transition reflects a change in the ligand field around the Fe site. Since we are discussing the case of second-ML Fe-phen molecules, this reflects a change in angle between the NCS branches [see Fig. 3(d)].

(a) As previously discussed, the topographical changes could originate from orbital changes. In that case, the energy position of the orbital should not vary much with the tunneling current. Exceptions are found by Gopakumar *et al.* [33,34], who observe that the HOMO or LUMO of phthalocyanine molecules can be slightly shifted by the electric field. However, the shifts were towards the Fermi level modeled with a capacitor interface. Yet, referring to Fig. 8(d), the orbital shift would be towards higher energies with increasing electric field (i.e., tunneling current), which does not fit this capacitor model.

(b) The observed transition could also be ascribed to the expected spin transition. The molecule would go from a HS state at low voltages characterized by an interlobe distance ≈ 7.6 Å to a LS state at higher voltages with an interlobe distance ≈ 6.0 Å. Why, then, is the spin transition, as quantified by the change in interlobe distance, proceeding smoothly with applied bias voltage, rather than abruptly as we found for first-ML Fe-phen on CuN [15]? Indeed, referring to Fig. 8(c), intermediate interlobe distances are observed. We propose that the observed interlobe distance represents the time-averaged distance corresponding to a molecule spending α proportion of time in the HS state and $1 - \alpha$ proportion of time in the LS state. This leads to an interlobe distance expressed as

$$d = \alpha(d_{HS} - d_{LS}) + d_{LS}. \quad (2)$$

This means that, during the measurement time of a single STM height profile (about 8 s), the investigated molecule has time to switch its spin state many times.

If we assume spin-state switching to occur in both directions, the time derivative of the time proportion in the HS state

α is then

$$\frac{d\alpha(t)}{dt} = -\alpha S_{\text{HS} \rightarrow \text{LS}}(I, V) + (1 - \alpha) S_{\text{LS} \rightarrow \text{HS}}(I, V), \quad (3)$$

which involves the switching rates $S_{\text{HS} \rightarrow \text{LS}}(I, V)$ [$S_{\text{LS} \rightarrow \text{HS}}(I, V)$] from HS to LS (LS to HS). In the stationary regime, Eq. (3) leads to

$$\alpha(I, V) = \frac{S_{\text{LS} \rightarrow \text{HS}}(I, V)}{S_{\text{LS} \rightarrow \text{HS}}(I, V) + S_{\text{HS} \rightarrow \text{LS}}(I, V)}. \quad (4)$$

As expected from our hypothesis, Eq. (4) describes how, for a given voltage and tunneling current, the molecule can spend a given proportion of time in the HS state and the rest of the time in the LS state, leading to an averaged distance between the lobes d given by Eq. (2). Equation (4) also describes how a competition between the current- and voltage-dependent switching rates [$S_{\text{HS} \rightarrow \text{LS}}(I, V)$ and $S_{\text{LS} \rightarrow \text{HS}}(I, V)$] affects the proportion of time spent in a given spin state. In turn, this would explain the tunneling current dependence on the threshold voltage observed in our experiments [see Fig. 8(d)]. Within this formalism, the points of Fig. 8(d) represent the set of I and V for which the switching rates are equal.

Several mechanisms may account for the rapid switching between spin states that we propose to have observed. First, as discussed previously, we believe in the existence of a potential energy barrier between the two spin states that originates from the adsorption site and we believe that the barrier becomes much lower in the case of a phen-phen bonding (second ML) compared to S-Cu bonding (first ML). Thus, although the measurements are realized at low temperature, we should consider “direct switching” as a possible switching mechanism where the switching rates are given by the transition-state theory (Arrhenius law). This mechanism is schematized in Fig. 9 where $w_{\text{HS} \rightarrow \text{LS}}$ and $w_{\text{LS} \rightarrow \text{HS}}$ are the switching rates given by the transition-state theory for switching from HS to LS and LS to HS, respectively. These switching rates depend on the barrier heights (Δ_1 and Δ_2), which in turn depend on the energetic position of the HS and LS states that can be shifted, for instance, with an electric field [12,13,35–37]. Second, switching involving electron injection into an unoccupied molecular orbital state [15,16] should also be considered (see Fig. 9). We assume here that this single-electron process implies switching from the excited state (LS) to the ground state (HS) with a switching rate σI where σ is the inelastic process overall probability and I the tunneling current. We note that the linear dependence in current of this switching rate for the excited-state to the ground-state transition was demonstrated in Ref. [15] on the CuN/Fe-phen system, but the ground state was LS, so different from the actual HS ground state. In agreement with our phenomenological explanation, these mechanisms would both lead to switching rates that depend on the applied current and voltage: $s_{\text{LS} \rightarrow \text{HS}}(I, V) = w_{\text{LS} \rightarrow \text{HS}}(I, V) + \sigma I$ and $s_{\text{HS} \rightarrow \text{LS}}(I, V) = w_{\text{HS} \rightarrow \text{LS}}(I, V)$.

In the following, we will show that the picture of a dynamic spin transition governed by these two mechanisms is compatible with the experimental data shown in Fig. 8. We will exclude switching from HS to LS, induced by inelastic excitation as there would be no more agreement with the experimental data.

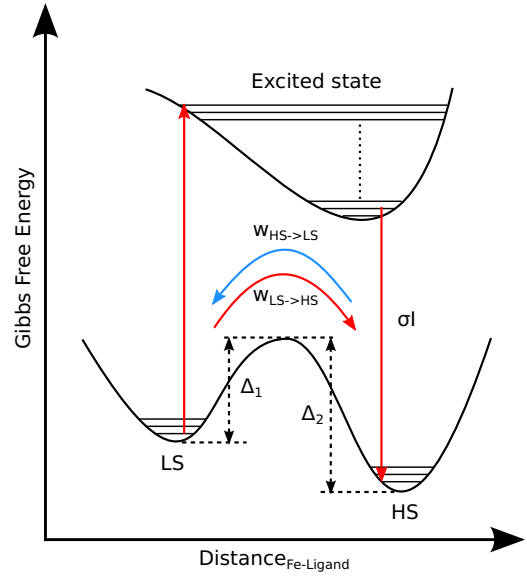


FIG. 9. (Color online) Suggested switching mechanisms for second-ML Fe-phen molecules on Cu(100). In this system, the HS state seems to be the ground state and thus has the lower Gibbs free energy. The energy barrier between the two spin states can be modified, for instance, by application of an electric field through the Stark effect and is low enough to allow switching given by the transition-state theory. In addition, we have a single-electron process with a cross section σ such as presented in Ref. [15] that allows switching from the LS to the HS state through an excited state.

C. Compatibility of the model with the experimental data

In this section, we use the switching mechanisms presented in Fig. 9 and derive the analytic form of the proportion of time spent into the HS state for a second-ML molecule as a function of the tunneling current and applied voltage [see Fig. 8(c)], and the current dependence of the voltage threshold [see Fig. 8(d)].

Within the scope of the transition-state theory, $w_{\text{LS} \rightarrow \text{HS}}(\text{HS} \rightarrow \text{LS})(I, V)$ are given by

$$w_{\text{LS} \rightarrow \text{HS}}(I, V) = \nu_0 \exp\left(-\frac{\Delta_1(I, V)}{k_B T}\right),$$

$$w_{\text{HS} \rightarrow \text{LS}}(I, V) = \nu_0 \exp\left(-\frac{\Delta_2(I, V)}{k_B T}\right), \quad (5)$$

where ν_0 is the attempt frequency assumed to be the same for both switching directions for simplicity, and Δ_1 (Δ_2) is the energy barrier to overcome for LS to HS (HS to LS) transition.

The energy levels of the HS and LS states and, consequently, the energy barriers Δ_1 and Δ_2 can vary with the applied electric field as the Stark effect leads to the addition of a potential energy in the form [38]

$$U_{\text{HS(LS)}} = -\mu_{\text{HS(LS)}} E - \frac{1}{2} \alpha_{\text{HS(LS)}} E^2 \quad (6)$$

with $\mu_{\text{HS(LS)}}$ the static dipole moment and $\alpha_{\text{HS(LS)}}$ the polarizability tensor of Fe-phen in the HS (LS) state and E the electric field. We performed the following calculations using (a) the first term and (b) the second term in Eq. (6). While (a) and (b) lead to an overall agreement with the experimental data, the discrepancy is much smaller in the case of (b), especially for high electric fields. The better agreement observed for (b) can

be easily understood as, in our experiment, the electric fields we use have very high values, typically in the order 1 GV/m. Thus, in the following, we will only present the derivations obtained using (b). The Gibbs free-energy difference between the HS and the LS states is then expressed as

$$\Delta_2 - \Delta_1 = \epsilon_0 - \frac{1}{2}(\alpha_{LS} - \alpha_{HS})E^2 \quad (7)$$

with ϵ_0 the difference in Gibbs free energy between the LS and the HS states in the absence of electric field. Moreover, we approximate the electric field coming from the tip with the simple expression of the electric field of two parallel conducting plates $E = -\frac{V}{d}$. As the distance d between the tip and the sample varies logarithmically with the current, we develop E to the first order leading to an electric field proportional to the applied voltage $E \propto V$. We can thus rewrite Eq. (7) as

$$\Delta_2 - \Delta_1 = \epsilon_0 - \gamma V^2. \quad (8)$$

We can now express Eq. (4) as

$$\alpha = \frac{1 + \frac{\sigma}{v_0} \exp\left(\frac{\Delta_1}{k_B T}\right) I}{1 + \exp\left(-\frac{\epsilon_0 - \gamma V^2}{k_B T}\right) + \frac{\sigma}{v_0} \exp\left(\frac{\Delta_1}{k_B T}\right) I}. \quad (9)$$

Equation (9) gives, for a set of current and voltage, the proportion of time spent in the HS state for a second-ML molecule. If the current is kept constant, such as in a single experiment presented in Fig. 8(a), Eq. (9) predicts a decrease in the proportion of time spent in the HS state with increasing voltage that we propose to have observed in Fig. 8(c) through the reduction of the distance between the lobes. The voltage threshold V_{Th} is defined as the voltage at which half of the lobes' shrinking occurs [see Fig. 8(c)], and corresponds to $\alpha = \frac{1}{2}$. Within our interpretation of dynamic switching, V_{Th} has the following expression:

$$V_{Th} = \sqrt{\frac{\epsilon_0}{\gamma} + \frac{kT}{\gamma} \ln \left[1 + \frac{\sigma}{v_0} \exp\left(\frac{\Delta_1}{k_B T}\right) I_{sp} \right]}. \quad (10)$$

The analytic expression of the voltage threshold [Eq. (10)] is used to fit the experimental data of Fig. 8(d). There is a very good agreement between the experimental data and our simple dynamic-switching model. Moreover, the fitting parameters lead to $\frac{\epsilon_0}{\gamma} = 0.16 \pm 0.16$, $\frac{k_B T}{\gamma} = 0.044 \pm 0.730$, and $\frac{\sigma}{v_0} \exp\left(\frac{\Delta_1}{k_B T}\right) = 39.3600 \pm 0.0001$ (I being expressed in nA and V in V). Due to the fitting parameter uncertainties, we can only account for the order of magnitude of $\epsilon_0 \approx 1$ meV corresponding to the Gibbs free-energy difference between the LS and HS states in the absence of an electric field ($T \approx 4$ K).

The potential barrier height for a transition from the ground state to the excited state is higher than the corresponding energy difference between the states (e.g., for second-ML molecules, Δ_2 is larger than $G_{LS} - G_{HS} = \epsilon_0$). Thus, at low temperature, the low value of ϵ_0 , compared to the 170-meV energy difference between HS and LS of the Fe-phen free molecule calculated by Gueddida *et al.* [25], is consistent with the presence (absence) of the proposed dynamic switching for the second-ML (bulk) molecules.

To summarize this discussion, from the available experimental data, it is not possible to unambiguously prove that the observed topographical changes with increasing voltage are related to spin crossover. However, voltage-induced spin

crossover is intuitively expected on second-ML Fe-phen molecules considering our previous work [15] on first-ML molecules, and we have quantitatively shown that this effect can explain the experimental results, whereas probing a different orbital represents a less probable explanation. Indeed, if we were probing different orbitals, we would expect an energy shift towards the Fermi level with increasing electric field, i.e., a decreasing voltage threshold with increasing current instead of the observed voltage threshold increase with increasing current [Fig. 8(d)].

V. CONCLUSION

In conclusion, Fe-phen exhibits a layer-by-layer growth on Cu(100). Spin-state coexistence is observed for the first ML and the HS/LS proportion does not seem to be correlated with molecular coverage. We presume that commensurability considerations between the S-S distance, which drives the spin state of the Fe site, and the corrugated potential landscape of S adsorption sites promoted by the underlying Cu substrate, shall pin the spin state. This would explain the origin of the spin-state coexistence for the first-ML molecules. In contrast, second-ML Fe-phen molecules experience a weaker potential landscape from the underlying blanket of phen orbitals produced by the first-ML Fe-phen. This relaxes any commensurability constraints on the adsorption geometries of Fe-phen. We suspect that electronic considerations, such as phen-phen interactions, can then drive the second-ML Fe-phen into a HS ground state at low temperature. This HS ground state at low temperature for second-ML Fe-phen is in contrast to bulk Fe-phen's LS ground state.

We observe a bias-voltage-induced change in the distance of a second-ML molecule's two NCS groups that does not result in a metastable LS state at low bias. We presume that π - π interactions between the phenanthroline groups of the first and second ML of Fe-phen are much weaker than those arising from S-Cu bonding as experienced by the first ML of Fe-phen. Applying a bias voltage enables an apparent transition from HS to a steady-state combination of HS and LS states in a proportion that reflects the bias- and current-dependent switching rates to/from the HS state. This dynamic switching is supported by a model considering different switching mechanisms.

Based on the results obtained with the Fe-phen molecule, we provide, in the more general context of SCO complexes, key ingredients to (a) sustain the SCO property of the molecules by reducing the interaction with the substrate; (b) induce/suppress the metastability of the excited spin state; and (c) select the spin ground state of the molecules by using an adequate corrugation potential with commensurable adsorption sites provided by the substrate. We foresee at least two interesting perspectives. The first is to integrate or combine the properties of SCO ultrathin films within highly spin-polarized spinterfaces [39] for enhanced spintronic functionality. For example, we predict a bias-dependent increase in the efficiency of spin-polarized transport across a Fe-phen-based spintronic device due to the bias-induced analogic switchover from Fe-phen's HS to LS state. If the gate voltage of a three-terminal device is used to control this property separately, then this substrate- and bias-mediated engineering of the transition opens the path to

a spin-crossover-based molecular transistor [13] characterized by a continuum of conductance states between the HS- and LS-state extrema [15]. Combining these two perspectives should, in a third step, lead to a robust spin-based transistor.

ACKNOWLEDGMENTS

We thank G. Rogez for synthesizing the molecule, V. Da Costa for fruitful discussions, and S. Gueddida and M. Alouani

for sharing results before publication. We acknowledge funding from Franco-German university, from the Deutsche Forschungsgemeinschaft (DFG) within the Center for Functional Nanostructures (CFN) and the Baden-Württemberg Stiftung in the framework of the Kompetenznetz für Funktionale Nanostrukturen (KFN) and from the Agence Nationale de la Recherche ANR-09-JCJC-0137 and ANR-11-LABX-0058_NIE and from the International Center for Frontier Research in Chemistry.

-
- [1] K. Moth-Poulsen and T. Bjørnholm, *Nat. Nanotechnol.* **4**, 551 (2009).
- [2] S. J. v. der Molen and P. Liljeroth, *J. Phys.: Condens. Matter* **22**, 133001 (2010).
- [3] M. A. Halcrow, *Spin-Crossover Materials Properties and Applications* (Wiley, Chichester, UK, 2013).
- [4] E. König and K. Madeja, *Chem. Commun.* **3**, 61 (1966).
- [5] P. Gülich, Y. Garcia, and H. A. Goodwin, *Chem. Soc. Rev.* **29**, 419 (2000).
- [6] A. Bousseksou, G. Molnár, L. Salmon, and W. Nicolazzi, *Chem. Soc. Rev.* **40**, 3313 (2011).
- [7] H. J. Shepherd, G. Molnár, W. Nicolazzi, L. Salmon, and A. Bousseksou, *Eur. J. Inorg. Chem.* **2013**, 653 (2013).
- [8] A. Hauser, *Chem. Phys. Lett.* **124**, 543 (1986).
- [9] M. Marchivie, P. Guionneau, J. A. K. Howard, G. Chastanet, J. F. Létard, A. E. Goeta, and D. Chasseau, *J. Am. Chem. Soc.* **124**, 194 (2002).
- [10] K. Kato, M. Takata, Y. Morimoto, A. Nakamoto, and N. Kojima, *Appl. Phys. Lett.* **90**, 201902 (2007).
- [11] A. Bousseksou, G. Molnár, J. P. Tuchagues, N. Menéndez, É. Codjovi, and F. Varret, *C. R. Chim.* **6**, 329 (2003).
- [12] N. Baadji, M. Piacenza, T. Tugsuz, F. D. Sala, G. Maruccio, and S. Sanvito, *Nat. Mater.* **8**, 813 (2009).
- [13] V. Meded, A. Bagrets, K. Fink, R. Chandrasekar, M. Ruben, F. Evers, A. Bernand-Mantel, J. S. Seldenthuis, A. Beukman, and H. S. J. van der Zant, *Phys. Rev. B* **83**, 245415 (2011).
- [14] F. Prins, M. Monrabal-Capilla, E. A. Osorio, E. Coronado, and H. S. J. van der Zant, *Adv. Mater.* **23**, 1545 (2011).
- [15] T. Miyamachi, M. Gruber, V. Davesne, M. Bowen, S. Boukari, L. Joly, F. Scheurer, G. Rogez, T. K. Yamada, P. Ohresser, E. Beaurepaire, and W. Wulfhekel, *Nat. Commun.* **3**, 938 (2012).
- [16] T. G. Gopakumar, F. Matino, H. Naggert, A. Bannwarth, F. Tuczek, and R. Berndt, *Angew. Chem., Int. Ed.* **51**, 6262 (2012).
- [17] V. Davesne, M. Gruber, T. Miyamachi, V. Da Costa, S. Boukari, F. Scheurer, L. Joly, P. Ohresser, E. Otero, F. Choueikani, A. B. Gaspar, J. A. Real, W. Wulfhekel, M. Bowen, and E. Beaurepaire, *J. Chem. Phys.* **139**, 074708 (2013).
- [18] T. Mahfoud, G. Molnár, S. Cobo, L. Salmon, C. Thibault, C. Vieu, P. Demont, and A. Bousseksou, *Appl. Phys. Lett.* **99**, 053307 (2011).
- [19] S. Shi, G. Schmerber, J. Arabski, J. B. Beaufrand, D. J. Kim, S. Boukari, M. Bowen, N. T. Kemp, N. Viart, and G. Rogez, *Appl. Phys. Lett.* **95**, 043303 (2009).
- [20] H. Naggert, A. Bannwarth, S. Chemnitz, T. von Hofe, E. Quandt, and F. Tuczek, *Dalton Trans.* **40**, 6364 (2011).
- [21] T. Palamarciuc, J. C. Oberg, F. E. Hallak, C. F. Hirjibehedin, M. Serri, S. Heutz, J.-F. Létard, and P. Rosa, *J. Mater. Chem.* **22**, 9690 (2012).
- [22] A. Pronschinske, Y. Chen, G. F. Lewis, D. A. Shultz, A. Calzolari, M. Buongiorno Nardelli, and D. B. Dougherty, *Nano Lett.* **13**, 1429 (2013).
- [23] M. Bernien, D. Wiedemann, C. F. Hermanns, A. Krüger, D. Rolf, W. Kroener, P. Müller, A. Grohmann, and W. Kuch, *J. Phys. Chem. Lett.* **3**, 3431 (2012).
- [24] B. Warner, J. C. Oberg, T. G. Gill, F. El Hallak, C. F. Hirjibehedin, M. Serri, S. Heutz, M.-A. Arrio, P. Saintavit, M. Mannini, G. Poneti, R. Sessoli, and P. Rosa, *J. Phys. Chem. Lett.* **4**, 1546 (2013).
- [25] S. Gueddida and M. Alouani, *Phys. Rev. B* **87**, 144413 (2013).
- [26] S. Javaid, S. Lebègue, B. Detlefs, F. Ibrahim, F. Djeghloul, M. Bowen, S. Boukari, T. Miyamachi, J. Arabski, D. Spor, J. Zegenhagen, W. Wulfhekel, W. Weber, E. Beaurepaire, and M. Alouani, *Phys. Rev. B* **87**, 155418 (2013).
- [27] B. Gallois, J. A. Real, C. Hauw, and J. Zarembowitch, *Inorg. Chem.* **29**, 1152 (1990).
- [28] M. Reiher, *Inorg. Chem.* **41**, 6928 (2002).
- [29] L. Zhang, T. Miyamachi, T. Tomanić, R. Dehm, and W. Wulfhekel, *Rev. Sci. Instrum.* **82**, 103702 (2011).
- [30] K. Momma and F. Izumi, *J. Appl. Crystallogr.* **44**, 1272 (2011).
- [31] A. V. Sinititskiy, A. L. Tchougréeff, A. M. Tokmachev, and R. Dronskowski, *Phys. Chem. Chem. Phys.* **11**, 10983 (2009).
- [32] G. Félix, W. Nicolazzi, L. Salmon, G. Molnár, M. Perrier, G. Maurin, J. Larionova, J. Long, Y. Guari, and A. Bousseksou, *Phys. Rev. Lett.* **110**, 235701 (2013).
- [33] T. G. Gopakumar, F. Müller, and M. Hietschold, *J. Phys. Chem. B* **110**, 6060 (2006).
- [34] T. G. Gopakumar, J. Meiss, D. Pouladsaz, and M. Hietschold, *J. Phys. Chem. C* **112**, 2529 (2008).
- [35] M. Diefenbach and K. S. Kim, *Angew. Chem. Int. Ed.* **119**, 7784 (2007).
- [36] S. K. Shukla and S. Sanvito, *Phys. Rev. B* **80**, 184429 (2009).
- [37] A. Droghetti and S. Sanvito, *Phys. Rev. Lett.* **107**, 047201 (2011).
- [38] J. A. Stroschio and D. M. Eigler, *Science* **254**, 1319 (1991).
- [39] F. Djeghloul, F. Ibrahim, M. Cantoni, M. Bowen, L. Joly, S. Boukari, P. Ohresser, F. Bertran, P. Le Fèvre, P. Thakur, F. Scheurer, T. Miyamachi, R. Mattana, P. Seneor, A. Jaafar, C. Rinaldi, S. Javaid, J. Arabski, J.-P. Kappler, W. Wulfhekel, N. B. Brookes, R. Bertacco, A. Taleb-Ibrahimi, M. Alouani, E. Beaurepaire, and W. Weber, *Sci. Rep.* **3**, 1272 (2013).